J. Anat. (2003) **203**, pp223–233

Angiogenesis in the distal femoral chondroepiphysis of the rabbit during development of the secondary centre of ossification

M. R. Doschak,[1] D. M. L. Cooper,[2,3] C. N. Huculak,[1] J. R. Matyas,[2] D. A. Hart,[1] B. Hallgrimsson,[2] R. F. Zernicke[1] and R. C. Bray[1]

Departments of [1]Surgery, [2]Cell Biology and Anatomy, and [3]Archaeology, McCaig Centre for Joint Injury and Arthritis Research, Faculty of Medicine, University of Calgary, Alberta, Canada

Abstract

In the developing chondroepiphyses of long bones, the avascular cartilaginous anlage is invaded by numerous blood vessels, through the process of angiogenesis. The objective of this study was to investigate the chronology of this vascular invasion with the spontaneous calcification of the cartilaginous epiphysis during development of the secondary ossification centre in the rabbit distal femur. The time-course of chondroepiphyseal vascular invasion was determined histologically and standardized for eight gestational and four postnatal intervals by plotting kit body mass against crown–rump length. Similarly, microcomputed tomography (μ-CT) helped to visualize calcification at those same gestational and postnatal intervals. To confirm the angiogenic nature of the avascular chondroepiphysis, such samples were assayed on the chick chorio-allantoic membrane (CAM). Neovascular outgrowths from the CAM were apparent 48 h following introduction of an 18-day (gestational) chondroepiphyseal sample. Chondroepiphyseal samples were assayed for the potent developmental angiogenic factors bFGF and VEGF, with the mRNA expression for both these mediators being confirmed using RT-PCR. As angiogenesis and calcification during chondroepiphyseal development occur in a defined tissue environment initially devoid of blood vessels and mineral, those processes provided a unique opportunity to study their progression without complication of injury-related inflammation or extant vasculature and mineral. Furthermore, the discovery of angiogenic, angiostatic or mineral-regulating mediators specific to developing connective tissue may prove useful for analysing the regulation of vascular and mineral pathogenesis in articular tissues.

Key words bFGF; cartilage canals; chorioallantoic membrane; matrix mineralization; μ-CT.

Introduction

Adult articular cartilage is avascular but, during embryological development, blood vessels invade and vascularize cartilage of the epiphyseal long bones. The development of these vessels found in cartilage erosions (canals) has been described morphologically and involves a stepwise neovascularization of the epiphysis that terminates with the establishment of a centrally located secondary centre of ossification (Moss-Salentijn, 1975; Floyd et al. 1987; Ganey et al. 1992; Skawina et al. 1994). Confluent blood vessels meeting in the centre expand to form a cavitation by the erosion of surrounding cartilaginous matrix. Spontaneous calcification of the epiphyseal matrix begins as the secondary centre of ossification forms. Matrix mineralization proceeds from multiple central nidi and radiates out towards the periphery, leaving only a surface veneer of unmineralized articular cartilage.

Angiogenesis proceeds as a series of distinct events from endothelial cell activation and migration, to the formation of patent new blood vessels (Sandison, 1928; Ausprunk & Folkman, 1977; Colville-Nash et al. 1995). Angiogenesis is often present amidst the inflammatory

Correspondence
Michael Doschak, MSc, c/o Dr Robert C. Bray, The University of Calgary, 3330, Hospital Drive NW, Calgary, Alberta, Canada T2N 4 N1. Tel.: +1 (403) 220 7866; fax: +1 (403) 270 0617; e-mail: doschak@ucalgary.ca

Accepted for publication *6 May 2003*

mediators of arthritic conditions (Brown & Weiss, 1988), and thus the regulatory molecules of angiogenesis are difficult to discern from those of the inflammatory response. As the general features of capillary growth are similar regardless of the source of the angiogenic stimulus (Folkman, 1986), the developmental process of angiogenesis in the cartilage canals of the fetal New Zealand White (NZW) rabbit provides an opportunity to observe the angiogenic process in joint connective tissues, without the presence of underlying inflammation, injury or extant vasculature.

The objectives of this study were to: (1) establish the time-course of vascular invasion in the distal femoral chondroepiphysis of the NZW rabbit, (2) investigate the chronology of these vascular events with the spontaneous calcification of the cartilaginous epiphysis during development of the secondary ossification centre and (3) confirm the expression of angiogenic factors resident within the local environment of the chondroepiphysis during development of the secondary ossification centre.

Materials and methods

Experimental design and animal handling

The time-course and chronology of vascular invasion and calcification were established using gross physical measurements, histological evaluation and microcomputed tomography (μ-CT). As the physical presence of blood vessels may result through vessel inclusion during radial growth of the avascular cartilage, the chorioallantoic membrane assay was employed to demonstrate the temporal expression of an angiogenic stimulus. Reverse transcription – polymerase chain reaction (RT-PCR) was used to identify angiogenic factors.

Fifteen 6-month-old, pregnant female NZW rabbits were used, and a total of 102 kits (from those rabbits) were evaluated at eight gestational (18, 19, 20, 21, 25, 26, 29 and 30 days) and four postnatal newborn (NB) intervals (NB1, NB4, NB8, NB11, and NB17 d). Animals were purchased from a single supplier (Riemens Fur Ranches, St Agathe, Ontario, Canada) and were housed individually in wire bottomed cages ($65 \times 40 \times 45$ cm; length $\times$ width $\times$ height). Unrestricted cage activity was allowed and a 12 : 12 h light–dark cycle was simulated in a quiet room at 20 °C. Water and standard laboratory rabbit chow were permitted *ad libitum*. The Faculty of Medicine Animal Care Committee reviewed and approved the experimental protocol based on established criteria of the Canadian Council on Animal Care (CCAC, 1994).

Pregnant rabbits were timed from the suspected hour of insemination, which occurred through the regular mating of 6-month-old virgin females with a male breeder. The pregnant rabbits were killed by intravenous injection of barbiturate. Litters were delivered through an abdominal dissection, and placed on a covered warming mat set at 39 °C.

Measures of temporal staging

The kits, which numbered from four to 11 per litter, were initially weighed, and crown–rump (C-R) length was measured, using a piece of thread referenced against a graduated ruler. Body mass and C-R length were compared with age (number of days post-insemination). Results were graphically displayed, and the gestational age for subsequent evaluations was determined from the graph as mass vs. C-R length. The kits were killed by decapitation or by lethal injection. The hind limbs were severed at the hip with a scalpel and fixed in a picric acid/4% paraformaldehyde fixative.

Histological evaluation of cartilage canals and immunohistochemistry

The entire hind limb from one kit, at each developmental time point, was serially sectioned at 20 μm using a cryomicrotome. Temporal assessments of cartilage canal progression were made with respect to the formation of the secondary ossification centre in the central epiphysis, in conjunction with evidence of calcification – visible as dense granules in the cellular cartilaginous matrix.

Representative slides at each time point were subsequently stained using antithrombomodulin (a molecule expressed on the luminal surface of endothelial cells) immunohistochemistry to discern morphologically the blood vessels from surrounding connective tissue (Bourin, 1991). Few common endothelial cell markers are commercially available for rabbit tissue antigens. Thus we chose to use an antirabbit thrombomodulin antibody to identify blood vessels as we have validated this reagent in a previous study (Doschak et al. 2001).

Sections were blocked with 5% bovine serum albumin and pre-incubated with normal rabbit serum. Sections were incubated with goat antirabbit thrombomodulin (Drs C. and N. Esmon, Oklahoma Medical Research Foundation, Oklahoma City, OK, USA) for 48 h at 4 °C.

Following rinses in PBS/0.1% Triton-X 100, sections were reacted with secondary rabbit antigoat IgG FITC conjugate for 1 h at room temperature in the dark. Following final rinses, sections were mounted and examined under epifluorescent illumination (Leitz Orthoplan microscope, Leica Inc., BC, Canada). Those same sections were then stained with haematoxylin and eosin for complete morphological assessment. Photomicrography was performed using an Orthomat camera housing attachment (Leica) with high-speed (400 ASA) colour slide film.

μ-CT of calcified mineral

To map the formation of mineralized bone, fixed rabbit kit hindlimbs were disarticulated at all time points, and the entire knee joint was scanned using an X-ray microtomograph (μ-CT, SkyScan 1072, Aartselaar, Belgium). The limbs were scanned at 100 kV through 180° with a rotation step of 0.9°. All samples were scanned at ×12 magnification that produced serial cross-sectional images composed of isotropic 19.4-mm^3 voxels. Scion Image, beta 4.0.2 (Scion Image Corporation, USA) was used to median-filter the raw image data to reduce noise. The filtered image data were then exported to ANALYSE™ 4.0 (Mayo Clinic, Rochester, MN, USA) for volumetric rendering.

Chorio-allantoic membrane transplantation experiments

To confirm the temporal expression of angiogenic factor(s), four chicken eggs were obtained and prepared at 13 days post-fertilization to accept fetal rabbit chondroepiphyseal transplants 1 day prior to vascular invasion.

The blunt end of each egg was scored and pierced, and the fibrous air sac membrane peeled back to expose the patent chorio-allantoic membrane (CAM). Four kits, at 19 days post-insemination, were isolated aseptically and delivered into sterile Petri-dishes lined with sterilized filter paper. The kits were weighed, and the C-R length measured prior to decapitation. The femur was dissected free under a dissecting scope by teasing the sample over the dry filter paper. Once isolated, the distal femoral epiphysis was severed with a scalpel blade just below the condylar curvature, close to the growth plate region. The sample was moistened with chick Ringer's solution, and transplanted onto the CAM (Selleck, 1996). The eggs were incubated in a rotating dry-air 37 °C egg incubator. Following incubation from 1 to 4 days post-implantation, the samples were exposed and photographed, and fixed for sectioning, as described previously.

RT-PCR

To test for the expression of known developmental angiogenic factors within the avascular chondroepiphyseal sample, RNA was extracted from pooled samples of severed chondroepiphyses from 19 days of gestation to the first day after birth (birth being *c*. 30 days of gestation). Samples were severed transversely with a scalpel blade after microdissection and did not include the growth plate.

RNA extraction

Total RNA was isolated using the well-documented TRIspin method (Reno et al. 1997). Briefly, tissue samples at each interval were massed, pooled, flash frozen in liquid nitrogen and dismembrated using a Braun microdismembrator (Mikro-Dismembrator S, B. Braun Biotech International, Melsungen, Germany). Samples were homogenized in TRIzol (Gibco BRL, Gaithersburg, MD, USA), and RNA extracted using Qiagen Rneasy Mini Kits, where RNA sequences bind a silica-gel membrane while contaminants are washed through, before the RNA is eluted with a specialized low-salt buffer (Qiagen, Missisauga, Canada/Valencia, USA). Total yield/RNA sample was quantified flourometrically using the SYBRgreen II reagent (Molecular Probes, OR, USA) as described previously (Sciore et al. 1998).

Semiquantitative RT-PCR procedure

RT-PCR was performed as described previously (Sciore et al. 1998; Hellio Le Graverand et al. 2000). Briefly, copy DNA (cDNA) was synthesized from 1 μg of total RNA using the Omniscript Reverse Transcription kit (Qiagen/Valencia). All samples were converted to cDNA and subjected to PCR at the same time to avoid methodological variation. PCR reactions consisted of 2.5 units of *Taq* DNA polymerase, 200 μM of each dNTP and 1.5 mM of $MgCl_2$ in a final reaction volume of 50 μL. Amplification occurred under the following PCR conditions: β-actin: 94 °C for 30 s, 55 °C for 30 s, and 72 °C for 30 s; 30 cycles (Reno et al. 1997), bFGF: 94 °C for 30 s, 54 °C for 1 min, and 72 °C for 1 min and 30 s; 36 cycles (Viereck et al. 2002) and VEGF: 94 °C for 30 s,

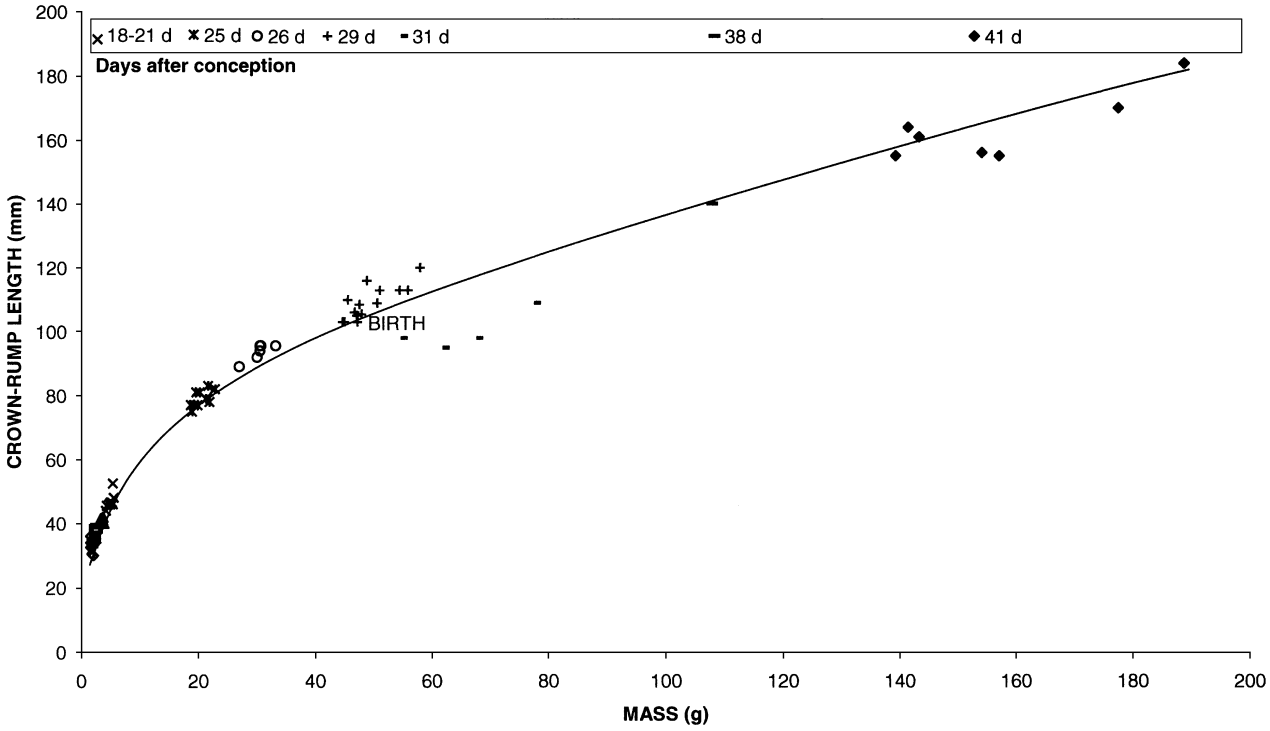

Fig. 1 Time-course of fetal New Zealand White rabbit growth, from 18 days of gestation, through birth at 30 days, to 11 days after birth. Kit crown–rump length was plotted against mass for each litter of rabbits killed. Litter ages (expressed as days after conception) are shown in the legend below the title.

58.6 °C for 2 min, and 72 °C for 30 s; 40 cycles (Kanzaki et al. 2002). PCR reactions were electrophoresed on 2% agarose gels, and visualized under ultraviolet light after staining with ethidium bromide. All no-RT controls (ie., RNA samples that did not undergo reverse transcription) were negative in the PCR reaction, indicating no genomic DNA contamination in the RNA preparations. PCR conditions and the image analysis system (Scanalytics) were in the linear range of detection.

Results

High variability existed in the body mass of kits delivered from the same litter and, presumably, at the same gestational age. C-R lengths varied accordingly, and when each kit mass was plotted as a function of C-R length, an exponential curve was obtained (Fig. 1). Plotted on log–log axes, the linear relationship accurately paralelled development.

Morphological vascular evaluations

Cartilage canal formation in the distal femur of the fetal rabbit began when vascular erosions penetrated the periphery of the chondroepiphysis (≈ 20 days of gestation) and was readily detected by 21 days. Erosions occurred simultaneously at multiple sites around the epiphysis, but commonly in the metaphyseal region of the epiphysis (Fig. 2a). The vascular components of the canal were seen centrally, and the advancing edge of vasculature appeared as a capillary glomerulus that burrowed into the cartilaginous anlage proceeding towards the centre of the epiphysis. Canals were often mushroom-shaped at their blind-ends, confirming a broad front of degradative enzymatic action at the advancing angiogenic edge. Anti-thrombomodulin immune-like reactivity highlighted the endothelial cells, not only in the epiphysis, but in the surrounding joint connective tissues such as ligament, tendon and bone (Fig. 2b). Cartilage canals progressed in number and distance from the epiphyseal periphery through to 29 days (Fig. 2c). The majority entered the epiphysis radially and extended linearly towards the centre. Deep within the centre of the epiphysis, canals were often seen entering through the intercondylar notch.

At 29 days, vessels began to meet in the epiphyseal centre, and the first signs of calcification appeared as dark granules under light microscopy (Fig. 2d),

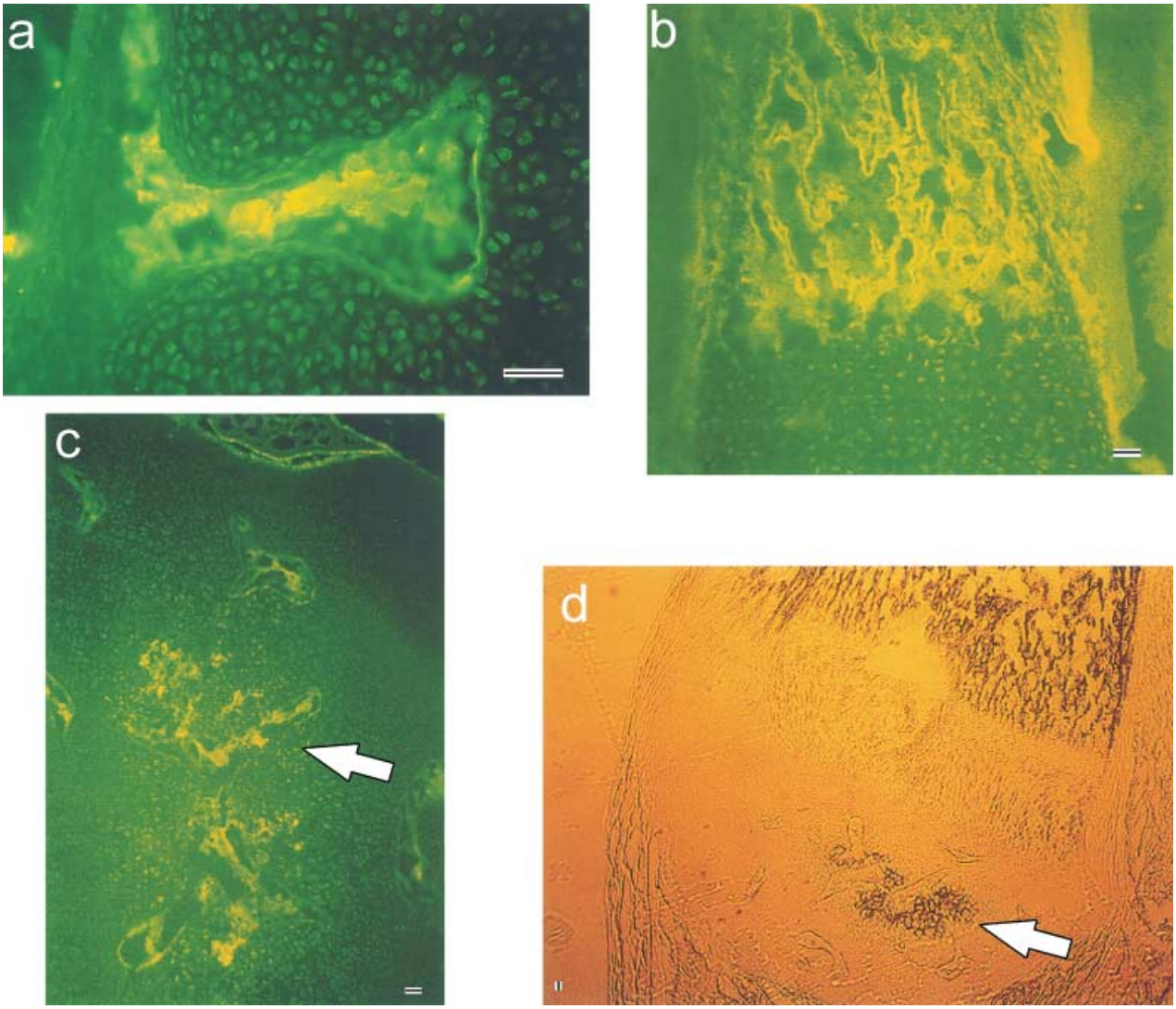

Fig. 2 Vascular material stained in the distal femoral chondroepiphysis using antithrombomodulin immune-like reactivity in: (a) 21 days of gestation metaphyseal cartilage canal erosion, (b) the mineralized diaphysis at 23 days of gestation and (c) the centrally forming secondary centre of ossification (arrow) at 29 days of gestation. Panel (d) illustrates the same frozen section at 29 days of gestation under bright-field transillumination, indicating black regions of calcified mineral (arrow), seen as multiple expanding nidi within the distal femoral chondroepiphysis and in the diaphysis. Scale bars = 50 μm.

originating centrally in the epiphysis. From day 29 through to birth (approximately day 30) and for a number of days afterwards, the secondary ossification centre formed as a cavitating process of central epiphyseal cartilage erosion and extensive calcification.

μ-CT evaluations

Mineralization of femoral cartilaginous anlage was first evidenced in the femoral diaphysis, where a hollow mineralized tube could readily be seen by 19 days of gestation (Fig. 3). The tube elongated rapidly in both directions and surrounded the nutrient foramen through an appositional mechanism, rather than through the union of multiple primary foci along the shaft. Fibular mineralization also appeared beside the tibial shaft. Bone mineral more than doubled in the first 1-day period, and the developing tibia paralleled the mineralization of the femoral diaphysis.

By 26 days of gestation, the mineralization fronts had progressed to the regions of the distal femoral and proximal tibial growth plates surrounding the future diarthrodial joint space. Both mineralized fronts appeared concave, consistent with apposition against a non-mineralized, rapidly expanding cellular mass. The mineralized fronts were also granular in consistency,

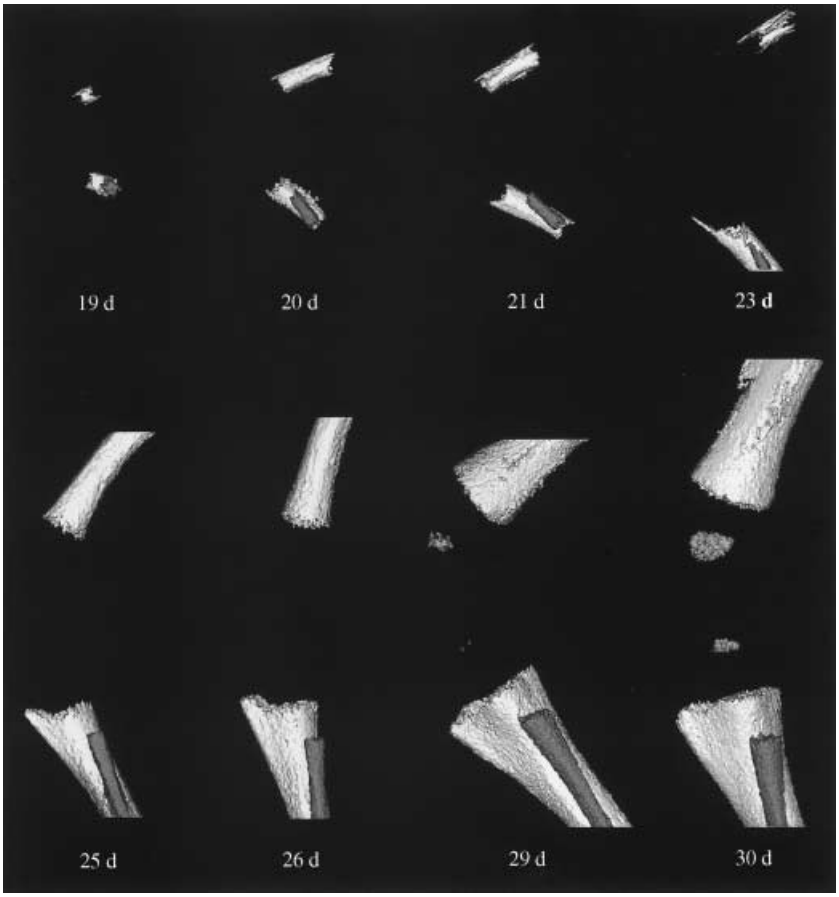

Fig. 3 Three-dimensional (3D) microcomputed tomography reconstructions of prenatal mineralization. Lateral view of the progression of mineralization in the skeletal structures of the left knee of the fetal New Zealand White rabbit. Gestational days are indicated. Joint integrity was maintained in all samples. All scans are presented at ×10 magnification, and the relative scale of the 3D reconstructions was consistent within the figure.

suggesting that the mechanism of mineral apposition was aggregational, rather than through lamellar processes.

By 29 days of gestation, mineral was clearly evidenced in the developing secondary centre of ossification. The origin of calcification occurred centrally and radiated outward to the periphery at subsequent time points. Characteristic architectural bony landmarks such as the tibial tubercle and metaphysis became evident. The fibular metaphysis was also developed by 30 days of gestation; however, it was positioned more distally to the joint than the tibial metaphysis, indicating its inferior attachment to the tibia via its non-mineralized, elongated chondroepiphysis. Mineralization continued appositionally around existing mineralized bone (diaphyseal and metaphyseal), resulting in radial growth of the newly modelled bone.

After birth, mineral deposition continued throughout the long bones, as indicated by their rapid growth (Fig. 4). The patella was not mineralized by 3–4 days after birth, but was clearly established at the later 17 days postnatal time-point. By 17 days postnatally, the mineralized epiphysis was in close position to the mineralized metaphysis, with only a thin layer of soft-tissue separating them at the growth plate. The calcified epiphyseal surface remained granular and was consistent with the secondary (epiphyseal) growth plate that underlay the remaining (but not visible) articulating cartilage.

Transplantation experiments

Four donor rabbit chondroepiphyses (19 days post-insemination) were overlaid onto the CAM of four donor eggs. They were subsequently removed and examined after 12 h (i.e. 19.5 days), 48 h (21 days), 72 h (22 days) and 120 h (24 days).

The first chondroepiphysis remained avascular after 12 h of contact with the CAM. The second chondroepiphysis appeared angiostimulatory when examined 48 h after introduction (Fig. 5a). New blood vessels sprouted from the surrounding CAM and grew directly toward and surrounded the chondroepiphysis (Fig. 5b). The chondroepiphysis was embedded within the collagenous

Fig. 4 Three-dimensional (3D) microcomputed tomography reconstructions of postnatal mineralization. Lateral view of the progression of mineralization in the skeletal structures of the left knee of the newborn (NB) New Zealand White rabbit. Days postnatal are indicated. Joint integrity was maintained in all samples, except in NB17 where it was approximated from two separate scans due to the large sample size. All scans are presented at ×9 magnification, and the relative scale of the 3D reconstructions was consistent within the figure (though scaled 25% smaller than the previous prenatal mineralization panel in Fig. 3).

matrix of the CAM, resulting in a living chimaeric construct. Microscopically, neovascularization was contained around the periphery of the chondroepiphysis. No vascular erosions penetrated the matrix of the chondroepiphysis, as usually witnessed in the embryological development in the fetal rabbit. Many nucleated chick blood cells were in proximity to the chondroepiphysis, and chick leucocytes were amassed in areas of vasculature surrounding the chondroepiphysis.

The third chondroepiphysis, examined at 72 h post-introduction, presented a very similar picture to that seen at 48 h, becoming surrounded by neovascular growths from the CAM (Fig. 5c,d). Microscopically, no vascular erosions were evidenced into the chondroepiphysis itself, but many small capillaries looped around and butted into the chondroepiphysis, suggesting temporally ongoing angiogenic stimulus. Chick leucocytes could be seen in association with the chondroepiphysis, and disintegration of epiphyseal structure was apparent. The final chondroepiphysis, examined 120 h post-introduction, had begun to fragment. Angiostimulatory growth surrounded the remnant chondroepiphyseal plugs, which had become incorporated into the chick CAM. No increase in epiphyseal size was noted, suggesting cessation of regulated developmental growth of the implant. Microscopically, viable chondrocytic nuclei were evident, but were surrounded by empty spaces and a decreased number of chondrocytes. Chick leucocytes surrounded the periphery of the plugs but were not observed in the remnant chondroepiphyseal implants.

RT-PCR

RT-PCR confirmed the expression of several potent angiogenic molecules from rabbit chondroepiphyseal samples at a number of developmental intervals assessed. The housekeeping gene, β-actin, was chosen to equalize gene expression between samples and demonstrated a 300-bp PCR product in all samples tested (Fig. 6a). Basic fibroblast growth factor (bFGF) expression was detected at all gestational and postnatal intervals tested. The PCR product of 275 bp was generated from chondroepiphyseal samples taken at 19, 20, 21, 23, 26 and 29 days, and the first day after birth (Fig. 6b). PCR primers were also designed for rabbit vascular endothelial growth factor (VEGF) and its four isoforms, which produced a primary PCR product at 646 bp and several other bands corresponding to expressed isoforms within the samples (Fig. 6c). Expression

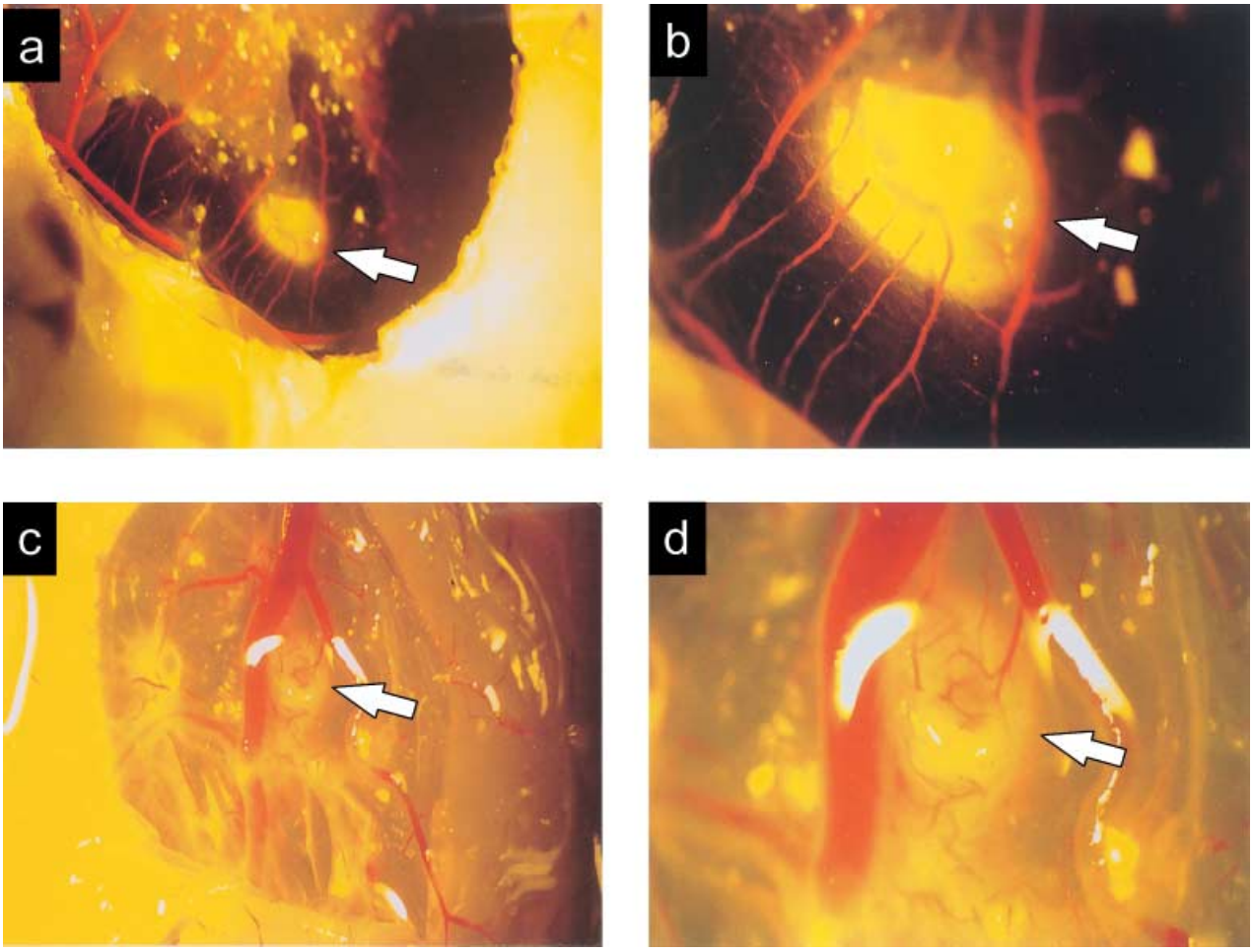

Fig. 5 Angiogenesis from the chick chorio-allantoic membrane directed toward a 48-h implant (magnifications ×5 and ×15.3 for a and b, respectively), and toward a 72-h implant (magnifications ×5 and ×15.3 for c and d, respectively) of 20 days of gestation fetal rabbit chondroepiphyseal explant. Arrows identify the implanted rabbit chondroepiphysis.

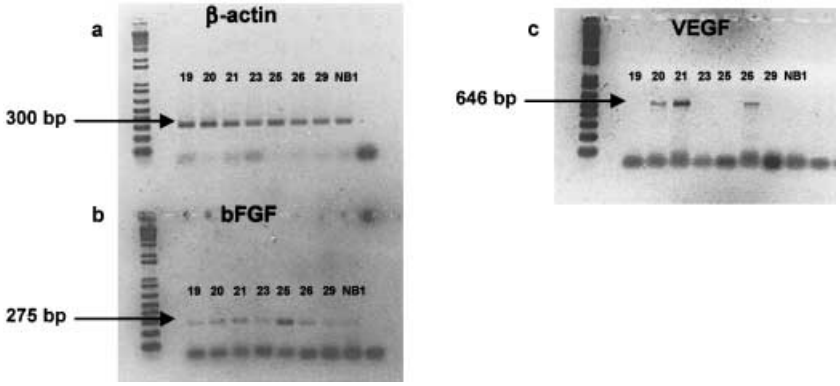

Fig. 6 Gene expression from samples of fetal rabbit chondroepiphyses, as determined by reverse transcription-polymerase chain reaction (RT-PCR). Samples were probed for (a) β-actin (PCR product of 300 bp), (b) basic fibroblast growth factor (bFGF; PCR product of 275 bp) and (c) vascular endothelial growth factor (VEGF; main PCR product of 646 bp) and its isoforms, and photographed on an ethidium-bromide-stained agarose gel. The gestational age of the fetal rabbit sample is indicated for each lane.

of VEGF was detected in our samples at 20, 21 and 26 days of gestation during our first PCR evaluations, confirming the expression of this angiogenic mediator during vascular invasion of the chondroepiphysis. Due to limitations in RNA in these tissues, a complete analysis of the temporal relations in the experimental model was precluded. Thus, the VEGF results should not be interpreted to infer VEGF temporal regulation without further experimentation.

Discussion

In this study, we investigated the time-course of developmental angiogenesis and mineralized bone formation in the distal femoral chondroepiphysis of the fetal NZW rabbit. At 20 days post-insemination, breaks in the continuity of the perichondrium were evident in the distal femoral head as blood vessels invaded the chondroepiphysis in response to angiogenic stimulus. Previous investigations have associated that event with a fetal body mass of 2.94 g (Ganey et al. 1992), and our investigation further defined that event at a C-R length of 22 mm. By 21 days, cartilage canals were apparent, and the vascular substance within those erosions stained positively with antithrombomodulin immune-like reactivity. Calcification was apparent, as the secondary ossification centre formed, and the blood vessels lay freely in the ossification centre once the cartilage was resorbed. With respect to bone formation, mineral was first evident in the diaphyseal shaft, and *de novo* at a later stage in the secondary centre of ossification.

Previous investigators have stressed the importance of a critical epiphyseal size, which triggered the onset of vascular invasion (Levene, 1964; Cole & Wezeman, 1987). Therefore, it was reasonable to hypothesize that some angiostimulatory molecule(s) were secreted by those cells once they reached a certain state of differentiation. Levene implantated autogenic rat chondroepiphyses into an incised flap of the rat kidney capsule, and demonstrated an angiogenic response toward the implant in one instance (Levene, 1960). Roach and coworkers previously cultured the explanted heads of femora and humeri from neonatal rabbits on the CAM to investigate the chronology of interactions between the vascular system and chondrocytes (Roach et al. 1998). Their investigation detailed the chick–host vascular interactions with the explanted rabbit chondrocytic cells and noted important interactions requiring the co-ordinated expression and secretion from both the vascular and the cartilage cell compartments, respectively. They noted, however, that using dissected explants from vascularized chondroepiphyses (i.e. at later stages of gestational and postnatal time points) resulted in a temporary ischaemia, which could lead to cell necrosis. Furthermore, the expression of angiogenic mediators may have originated from the resident vascular cells that had undergone an ischaemic trauma.

Here, we introduced 'avascular' chondroepiphyseal implants onto the CAM of an egg, a classical angiogenesis assay. As the avascular chondroepiphyses were probably small enough to derive nutrients by passive diffusion, the presence of severed vascular material was obviated, and the ischaemia of transplantation limited to seconds during translocation. Coinciding with the time-course for vascular invasion in the fetal rabbit chondroepiphysis, an angiostimulatory phenomenon was exerted by the implanted chondroepiphysis, and directed angiogenesis occurred in the CAM (Fig. 5). This phenomenon strongly supported the presence of a powerful angiogenic molecule(s) originating from the chondroepiphyseal cells during development.

To pursue further the identity of these molecules, we analysed the gene expression from chondroepiphyseal cells for the known angiogenic mediators bFGF and VEGF using RT-PCR. bFGF was expressed at all time periods sampled from 18 days of gestation to the first day after birth. Interestigly, the chondroepiphyseal cells expressed message for bFGF while still avascular (i.e. at 19 and 20 days) (Fig. 6b). Subsequently, mRNA expression for bFGF remained constant for the vascular developmental process associated with the secondary centre of ossification. We identified mRNA expression of VEGF and a number of its isoforms at several time points during chondroepiphyseal development, which suggested that this molecule played a regulatory role as well during vascular invasion and secondary centre formation. *In situ* hybridization studies will be required to determine accurately the identity of the cells that are actively secreting these angiogenic mediators, and to link their proximity to the developing vasculature.

As vascular elongation would be precluded by mineralized matrix, it was not surprising that angiogenic invasion occurred first and ahead of any mineralization events, which followed after vascular–chondrocytic interaction, particularly after chondrocyte hypertrophy (Ganey et al. 1995; Roach et al. 1998). Our μ-CT data

demonstrated two phases of mineral deposition closely following elongating blood vessels, first in the diaphyseal shaft as a hollow mineralized tube, and then centrally in the secondary centre of ossification once vascular processes had met. The chronology and association of vascular and chondrocyte matrix have been described in detail elsewhere, as has the perivascular cells in contact with the surrounding canal matrix (Moss-Salentijn, 1975; Cole & Wezeman, 1985). Large cylindrical spaces were evident in the forming mineral of the secondary ossification centres, indicating mineral proximity with pre-existing vascular substance, and resulting in the formation of morphological casts of the radiographically transparent vascular soft tissue. Calcification originated centrally, initially as one or more ossification nidi, and later radiated outward to the periphery, as previously reported (Trueta, 1957; Morini et al. 1999).

The mineralized fronts were granular in consistency, suggesting that the mechanism of mineral apposition was aggregational (i.e. depositional) rather than through a cell-mediated lamellar process as during bone remodelling. Our μ-CT investigations further characterized the developmental modelling of architectural long bone landmarks, such as the tibial tubercle and femoral and tibial metaphyses, and mineralized secondary centres. As the mineralization of both femoral and tibial secondary centres rapidly expanded toward the future joint space, and due to the lack of direct physical coupling with other than soft tissues, we inferred that bone modelling (at this phase of development) resulted through genetic factors, more so than through mechanotransductive stimuli. This view supported the skeletal patterning theories derived through descriptive embryology and anatomy in conjunction with paracrine factor regulation at the local level (Erlebacher et al. 1995). Furthermore, mineralization continued appositionally around existing mineralized bone (diaphyseal and metaphyseal), resulting in radial growth of the newly modelled bone, which similarly occurred without significant mechanotransductive stimuli.

Thus we observed that angiogenic and mineralization events in the developing articular chondroepiphysis were co-ordinated in a stepwise manner and occurred in response to the expression of resident stimulatory mediators. Developing cartilage canals provided a unique opportunity to observe the classical steps involved in angiogenesis and mineralization of long bones, without the complication of background pre-existing vessels and mineral or any underlying pathophysiology. The developmental system that was detailed in this study may therefore prove useful for studying angiogenic and mineralization processes in joint connective tissues, and elucidate natural cell mediators of regulatory control of those processes in disease.

Acknowledgments

We thank Dr Cyril Levene, Craig Sutherland and Chris MacKay. These studies were supported by grants from the Canadian Institutes of Health Research. Dr Ronald Zernicke is the Wood Professor in Joint Injury and Arthritis Research and Dr David Hart is the Calgary Foundation-Grace Glaum Professor in Arthritis Research. Dr Robert Bray is a Senior Scholar of the Alberta Heritage Foundation for Medical Research.

References

Ausprunk DH, Folkman J (1977) Migration and proliferation of endothelial cells in preformed and newly formed blood vessels during tumour angiogenesis. *Microvascular Res*. **14**, 53–65.

Bourin MC (1991) Thrombomodulin: a new proteoglycan. Structure–function relation. *Ann. Biol. Clin*. **49**, 199–207 (in French).

Brown RA, Weiss JB (1988) Neovascularization and its role in the osteoarthritic process. *Ann. Rheumatic Dis* **47**, 881–885.

CCAC (Canadian Council on Animal Care) (1994) *Guide to the Care and Use of Experimental Animals*, Vols 1 & 2. Ottawa, Ontario: CCAC.

Cole AA, Wezeman FH (1985) Perivascular cells in cartilage canals of the developing mouse epiphysis. *Am. J. Anat*. **174**, 119–129.

Cole AA, Wezeman FH (1987) Morphometric analysis of cartilage canals in the developing mouse epiphysis. *Acta Anat*. **128**, 93–97.

Colville-Nash PR, Alam CAS, Appleton I, Brown JR, Seed MP, Willoughby DA (1995) The pharmacological modulation of angiogenesis in chronic granulomatous inflammation. *J. Pharmacol. Exp. Therapeutics* **274**, 1463–1472.

Doschak MR, Matyas JR, Hart DA, Bray RC (2001) Vascular alterations in the rabbit patellar tendon after surgical incision. *J. Anat*. **198**, 513–523.

Erlebacher A, Filvaroff EH, Gitelman SE, Derynck R (1995) Toward a molecular understanding of skeletal development. *Cell* **80**, 371–378.

Floyd WE, Zaleske DJ, Schiller AL, Trahan C, Mankin HJ (1987) Vascular events associated with the appearance of the secondary centre of ossification in the murine distal femoral epiphysis. *J. Bone Joint Surg*. **69A**, 185–190.

Folkman J (1986) How is blood vessel growth regulated in normal and neoplastic tissue? *Cancer Res*. **46**, 467–473.

Ganey TM, Love SM, Ogden JA (1992) Development of vascularization in the chondroepiphysis of the rabbit. *J. Orthopaedic Res.* **10**, 496–510.

Ganey TM, Ogden JA, Sasse J, Neame PJ, Hilbelink DR (1995) Basement membrane composition of cartilage canals during development and ossification of the epiphysis. *Anat. Rec.* **241**, 425–437.

Hellio Le Graverand MP, Eggerer J, Sciore P, Reno C, Vignon E, Otterness I, et al. (2000) Matrix metalloproteinase-13 expression in rabbit knee joint connective tissues: influence of maturation and response to injury. *Matrix Biol.* **19**, 431–441.

Kanzaki Y, Onoue F, Ishikawa F, Ide T (2002) Telomerase rescues the expression levels of keratinocyte growth factor and insulin-like growth factor-II in senescent human fibroblasts. *Exp. Cell Res.* **279**, 321–329.

Levene C (1960) *The patterns of cartilage canals*. Doctoral thesis, University of Jamaica.

Levene C (1964) The patterns of cartilage canals. *J. Anat.* **98**, 515–538.

Morini S, Pannarale L, Franchitto A, Donati S, Gaudio E (1999) Microvascular features and ossification process in the femoral head of growing rats. *J. Anat.* **195**, 225–233.

Moss-Salentijn AGM (1975) *The epiphyseal vascularization of growth plates: a developmental study in the rabbit*. Doctoral thesis, University of Utrecht, Amsterdam, The Netherlands.

Reno C, Marchuk L, Sciore P, Frank CB, Hart DA (1997) Rapid isolation of total RNA from small samples of hypocellular, dense connective tissues. *Biotechniques* **22**, 1082–1086.

Roach HI, Baker JE, Clarke NM (1998) Initiation of the bony epiphysis in long bones: chronology of interactions between the vascular system and the chondrocytes. *J. Bone Mineral Res.* **13**, 950–961.

Sandison JC (1928) Observations on the growth of blood vessels as seen in the transparent chamber introduced in the rabbit's ear. *Am. J. Anat.* **41**, 475–496.

Sciore P, Boykiw R, Hart DA (1998) Semiquantitative reverse transcription-polymerase chain reaction analysis of mRNA for growth factors and growth factor receptors from normal and healing rabbit medial collateral ligament tissue. *J. Orthopaedic Res.* **16**, 429–437.

Selleck MAJ (1996) Culture and microsurgical manipulation of the early avian embryo. In *Methods in Cell Biology*, Vol. 51*; Methods in Avian Embryology* (ed. Bronner-Fraser M), pp. 1–20. San Diego: Academic Press.

Skawina A, Litwin JA, Gorczyca J, Miodonski AJ (1994) Blood vessels in epiphyseal cartilage of human fetal femoral bone: a scanning electron microscopic study of corrosion casts. *Anat. Embryol.* **189**, 457–462.

Trueta J (1957) The normal vascular anatomy of the human femoral head during growth. *J. Bone Joint Surg.* **39B**, 358–394.

Viereck V, Emons G, Lauck V, Frosch KH, Blaschke S, Grundker C, et al. (2002) Bisphosphonates pamidronate and zoledronic acid stimulate osteoprotegerin production by primary human osteoblasts. *Biochem. Biophys. Res. Commun.* **291**, 680–686.